

Functional characterization and transcriptional profiling of fibroblasts from patients with mutations in *SLC16A2* gene



Letizia Esposito^{1,2}, Federica Rey^{1,2}, Erika Maghraby^{1,3}, Letizia Messa^{2,4}, Fabio Bruschi^{5,6}, Gianvincenzo Zuccotti^{1,7}, Davide Tonduti^{5,6}, Stephana Carelli^{1,2,*}, Cristina Cereda^{2,7,*}

1 Pediatric Clinical Research Center "Romeo ed Enrica Invernizzi", Department of Biomedical and Clinical Sciences, University of Milan, Milan, Italy.
 2 Center of Functional Genomics and Rare Diseases, Department of Pediatrics, Buzzi Children's Hospital, Milan, Italy.
 3 Department of Biology and Biotechnology "L. Spallanzani", University of Pavia, Pavia, Italy.
 4 Department of Electronics, Information and Bioengineering (DEIB), Politecnico di Milano, Milan, Italy.

5 Unit of Pediatric Neurology, C.O.A.L.A. (Center for Diagnosis and Treatment of Leukodystrophies), V. Buzzi Children's Hospital, Milan, Italy
 6 Department of Biomedical and Clinical Sciences, University of Milan, Milan, Italy
 7 Department of Pediatrics, Children's Hospital "V. Buzzi", Milan, Italy.
 * These authors contributed equally to the work.

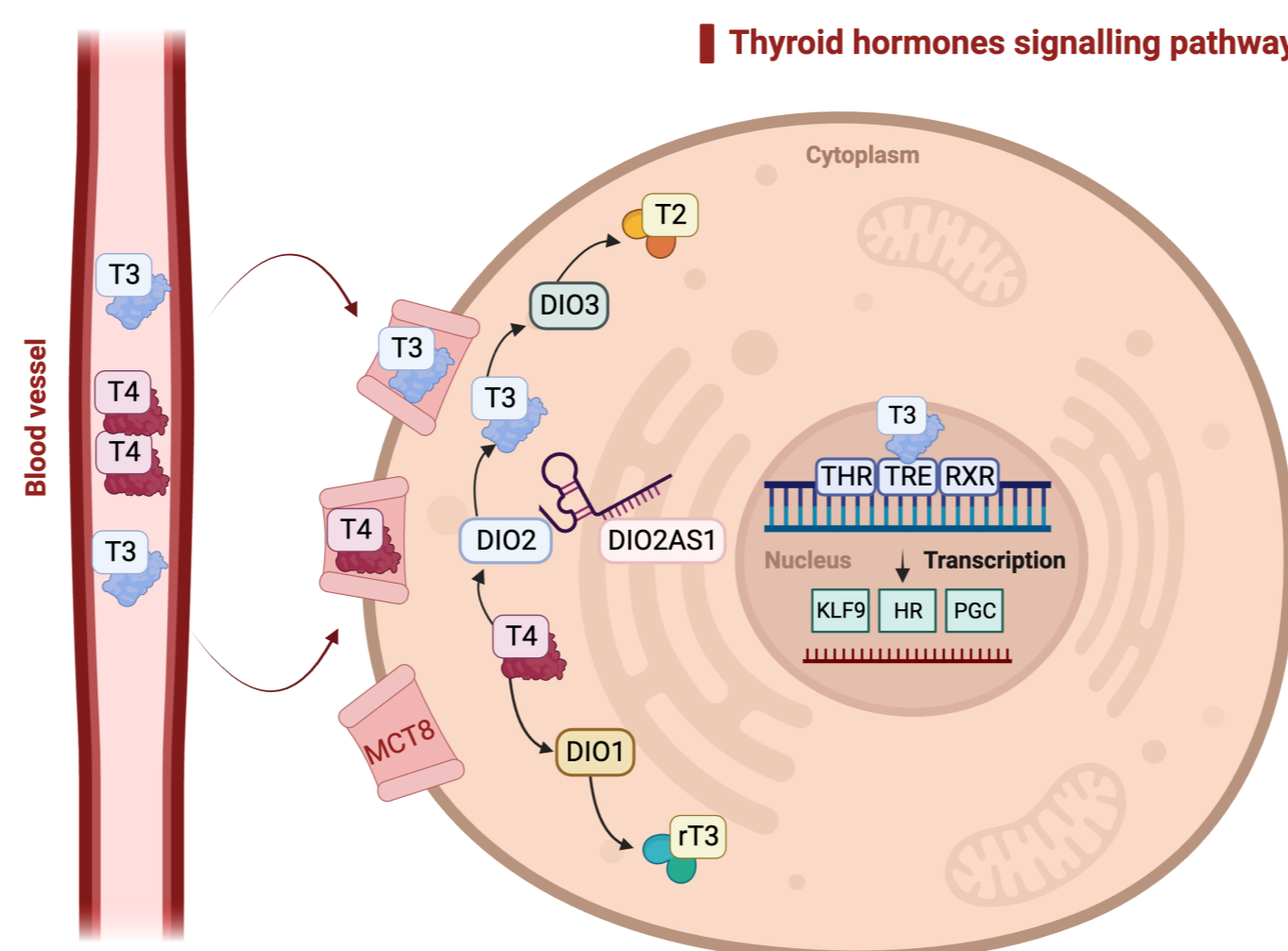
P20.049.B

Introduction

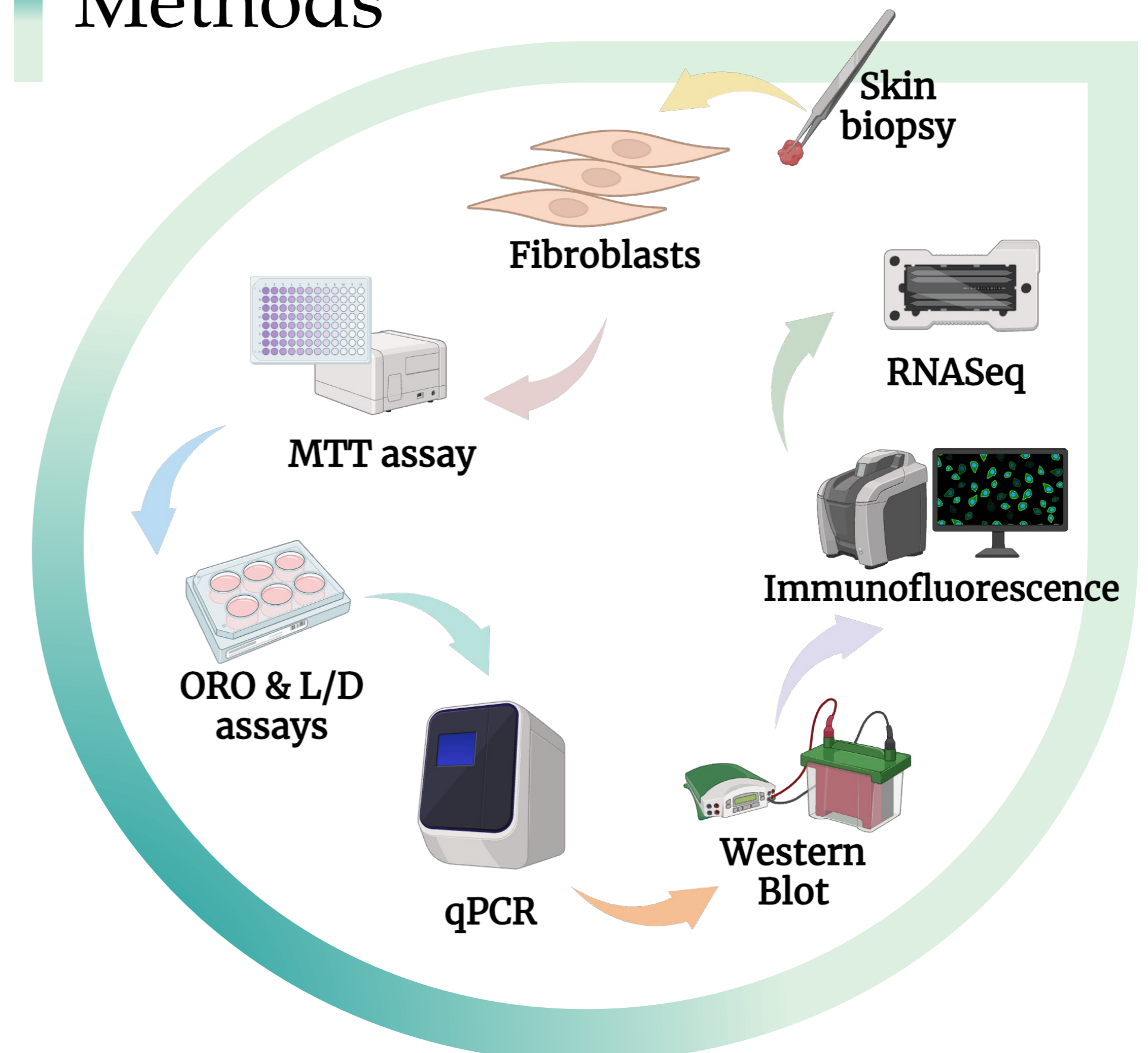
Genetics variants in *SLC16A2* gene encoding for the monocarboxylate transporter 8 (MCT8) cause a severe X-linked intellectual deficit known as Allan-Herndon-Dudley syndrome (AHDS). MCT8 promotes cellular uptake and efflux of thyroid hormones. Active T3 and retinoid X receptors (RXR) can form heterodimer complexes which bind to hormone response elements (HREs) that leads to activate or repress transcription.

Aim of the study

Our aim is to investigate the impact of MCT8 mutations on the pathogenetic mechanisms of AHDS.



Methods



Results

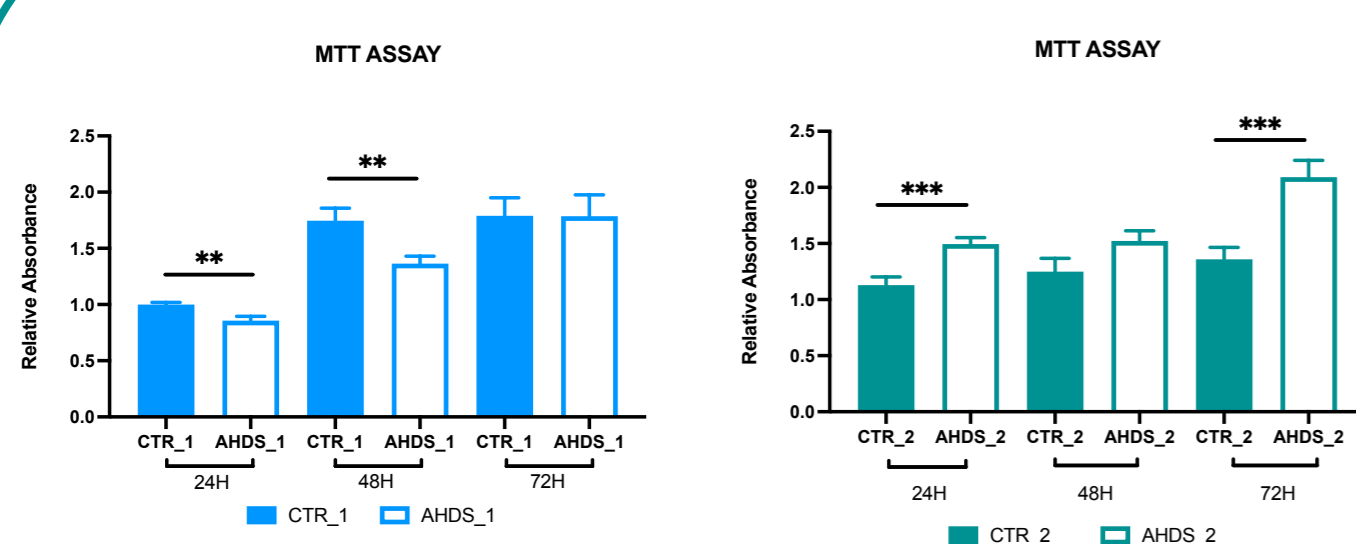


Figure 1. MTT assay after 24-48-72 hours (n=3, **p<0.01, ***p<0.001 vs CTR).

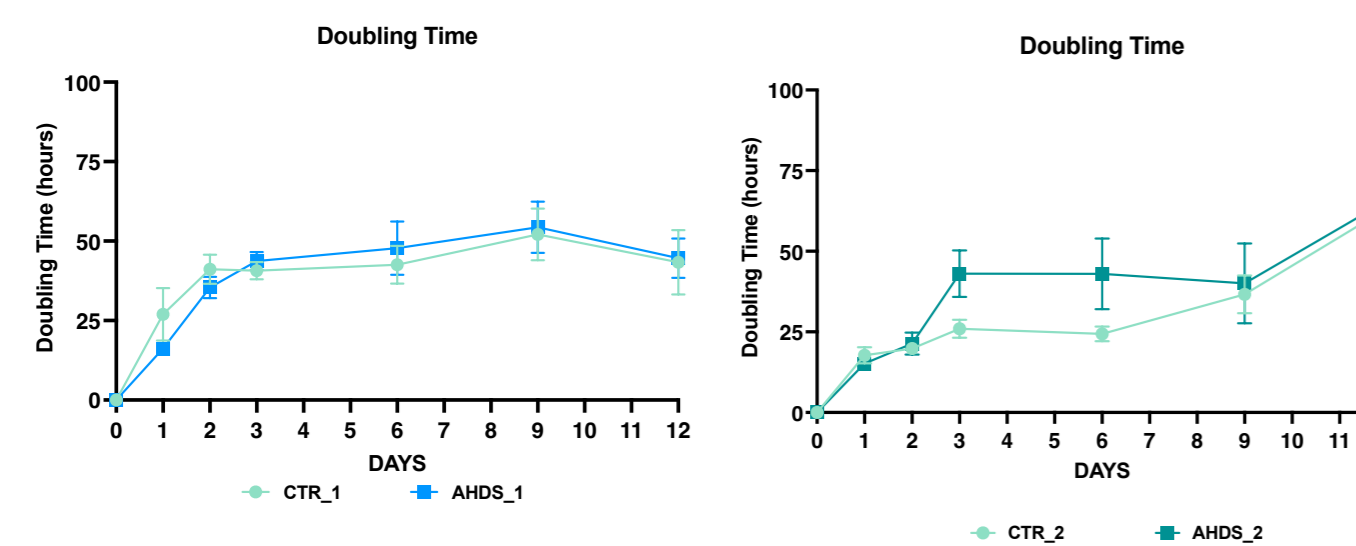


Figure 2. Doubling time for 1-2-3-4-6-12 days.

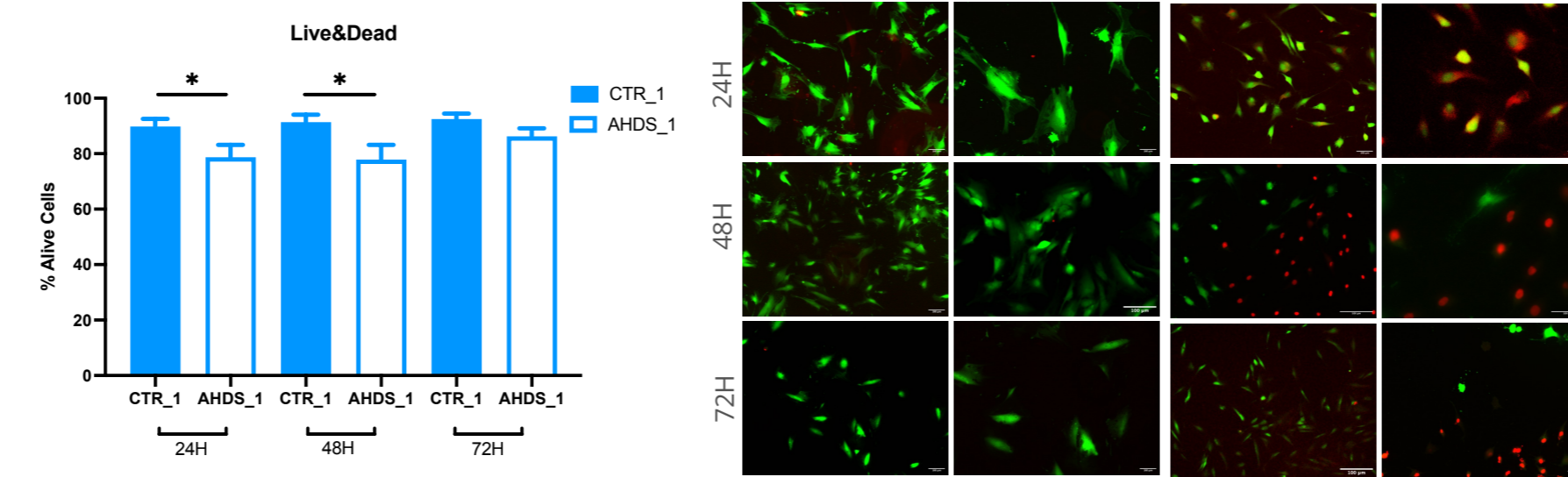


Figure 3. Live and Dead assay revealed a decrease in live cell populations (n=3, *p<0.05 vs CTR).

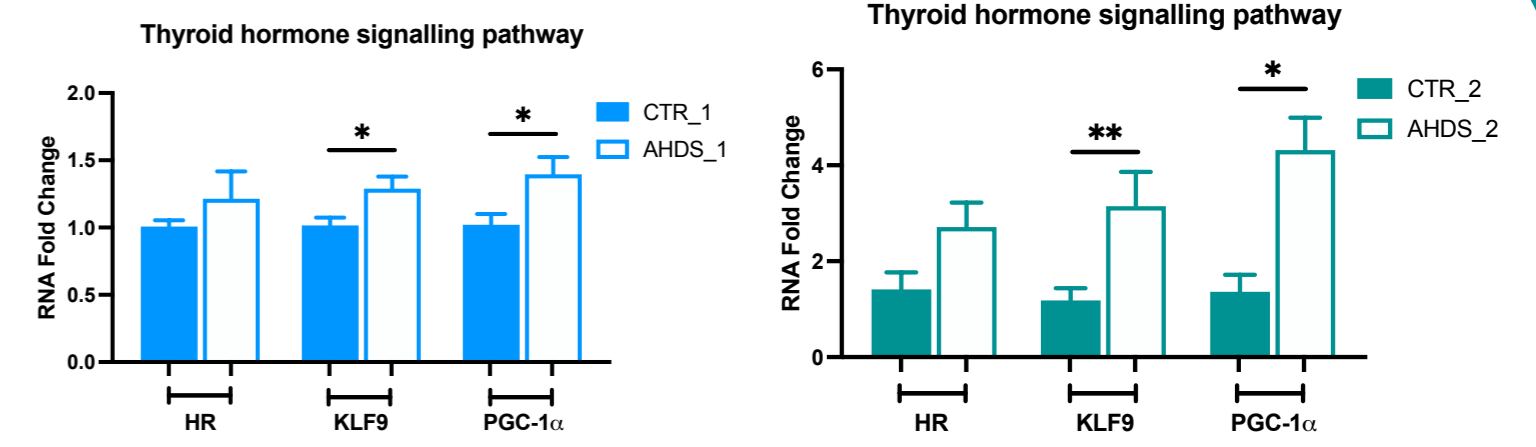
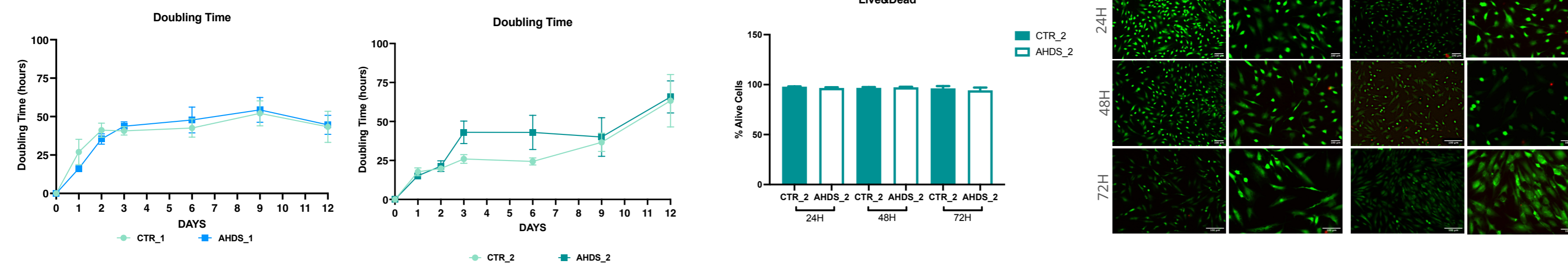


Figure 4. RT-PCR Analysis of thyroid hormone signalling pathway expression (n=3, *p<0.05, **p<0.01, ***p<0.001 vs CTR).

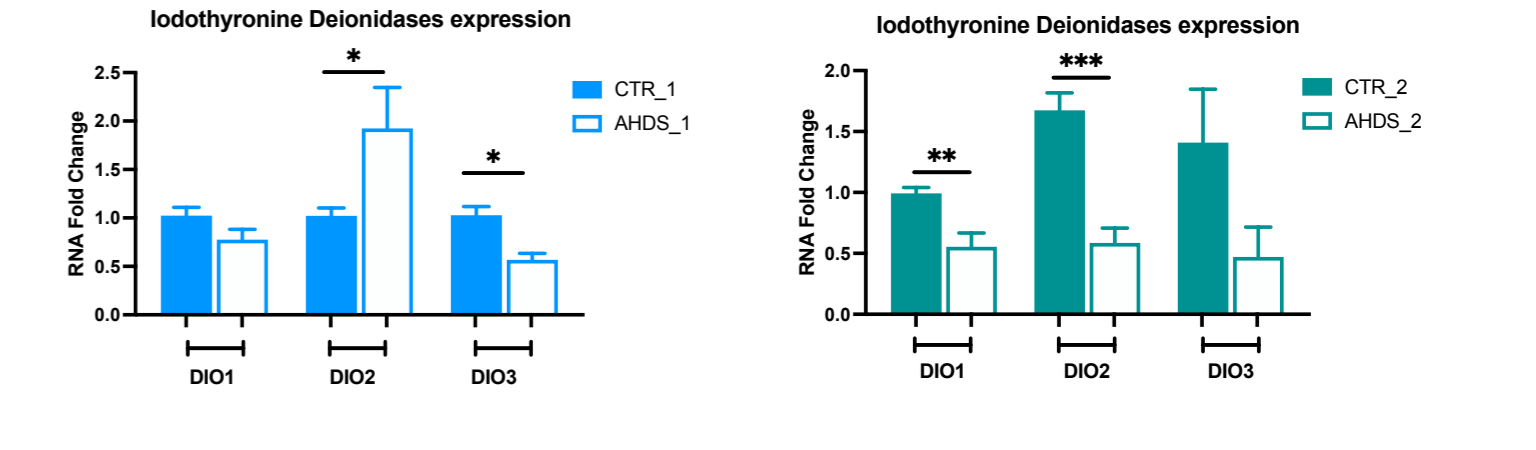
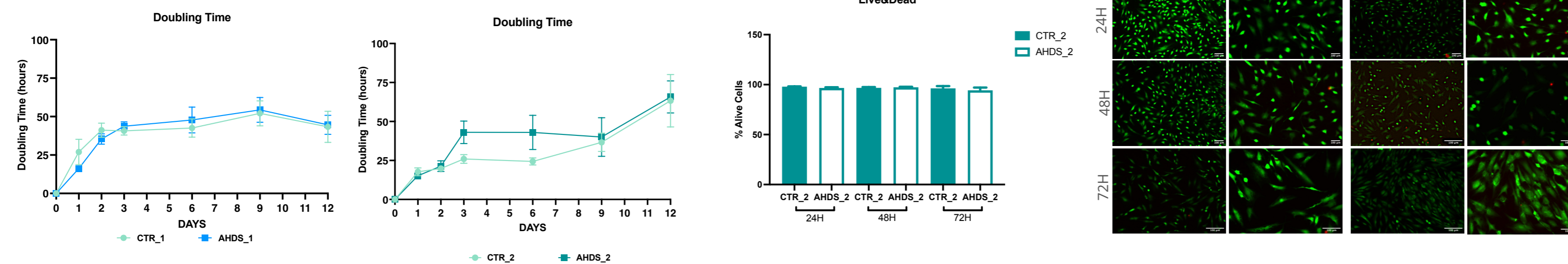


Figure 5. RT-PCR Analysis of iodothyronine Deionidases expression (n=3, *p<0.05, **p<0.01, ***p<0.001 vs CTR).

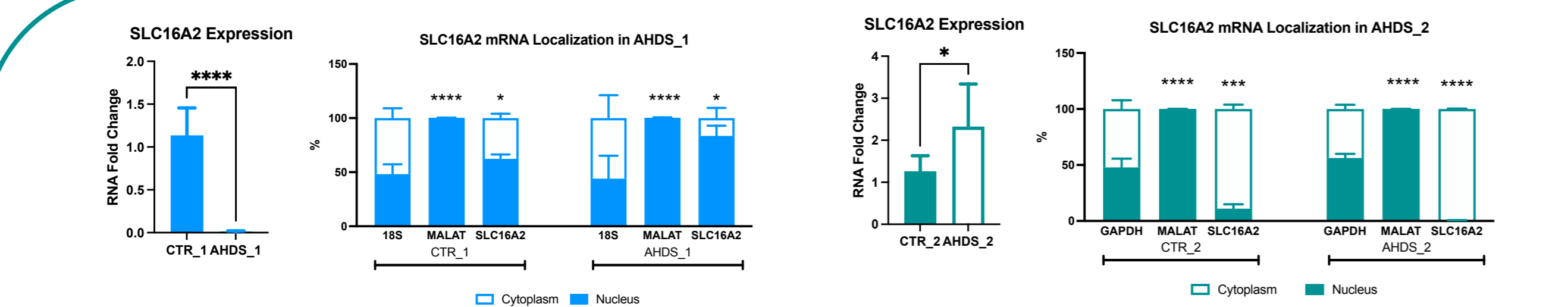


Figure 6. RT-qPCR Analysis of both SLC16A2 expression and localization (n=3, *p<0.05, ***p<0.001, ****p<0.0001 vs CTR).

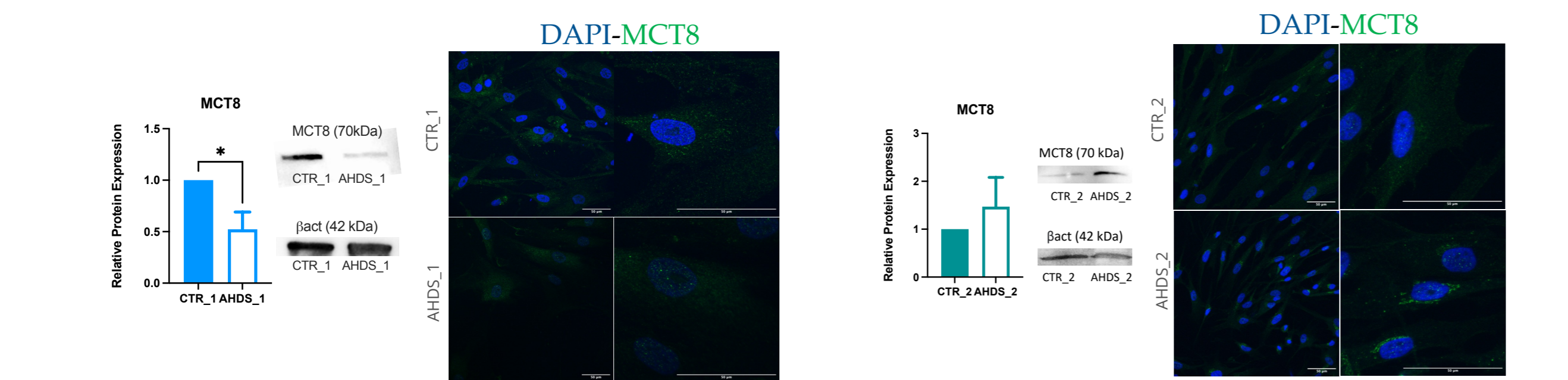


Figure 7. MCT8 expression via western blot and immunofluorescence (n=3, *p<0.05 vs CTR).

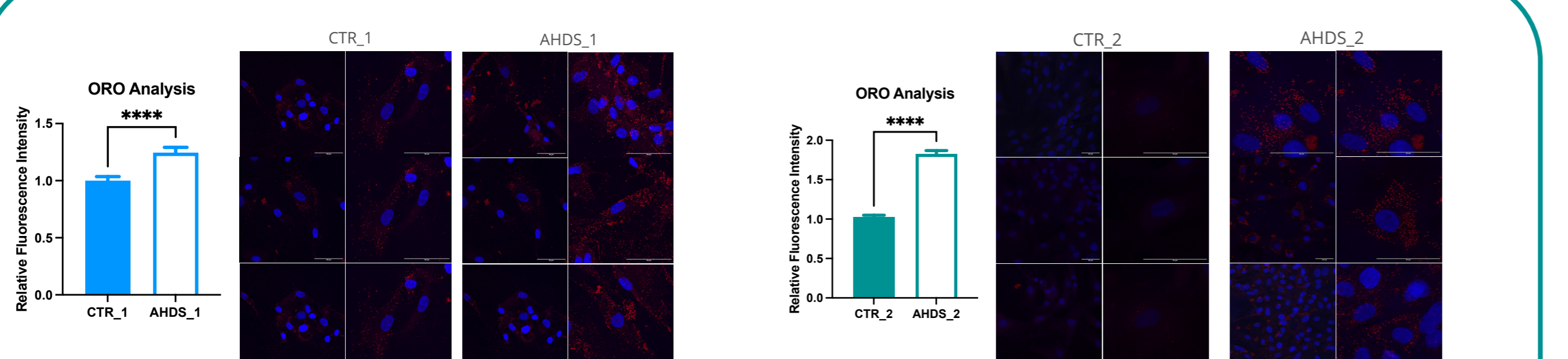


Figure 8. The Oil Red O staining revealed an increasing presence of lipid droplets (****p<0.0001 vs CTR).

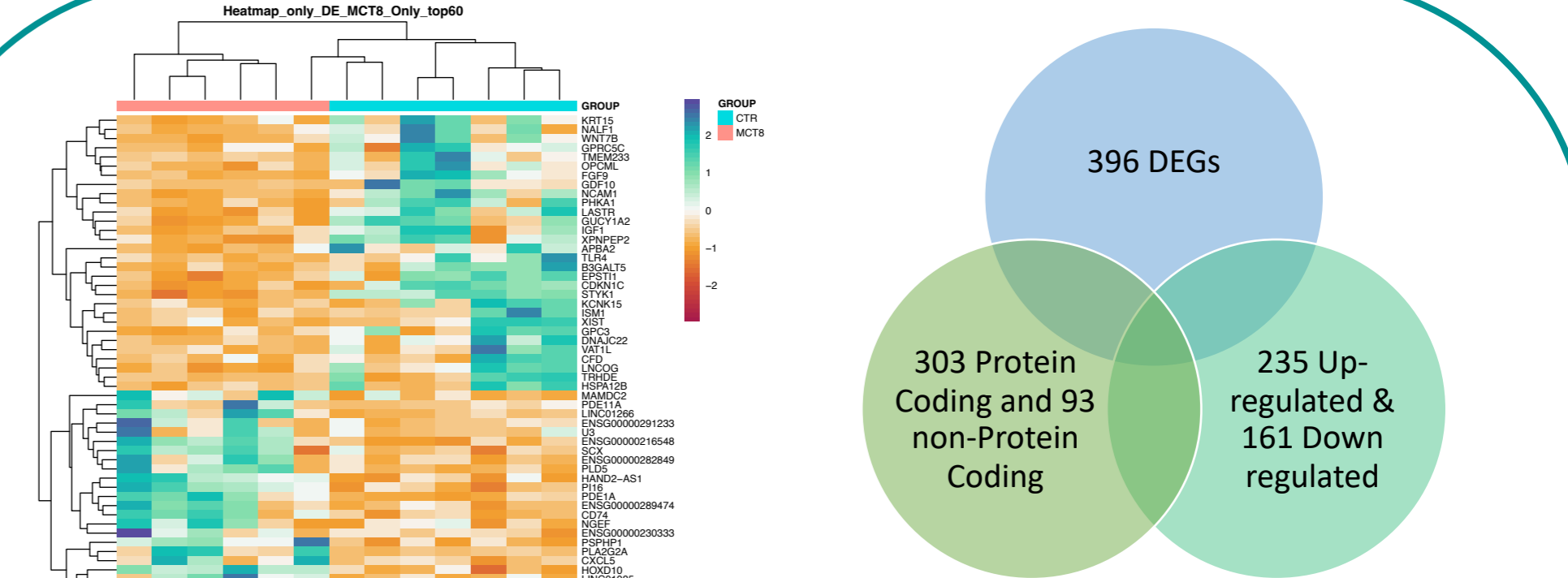


Figure 9. Heatmap of DEGs

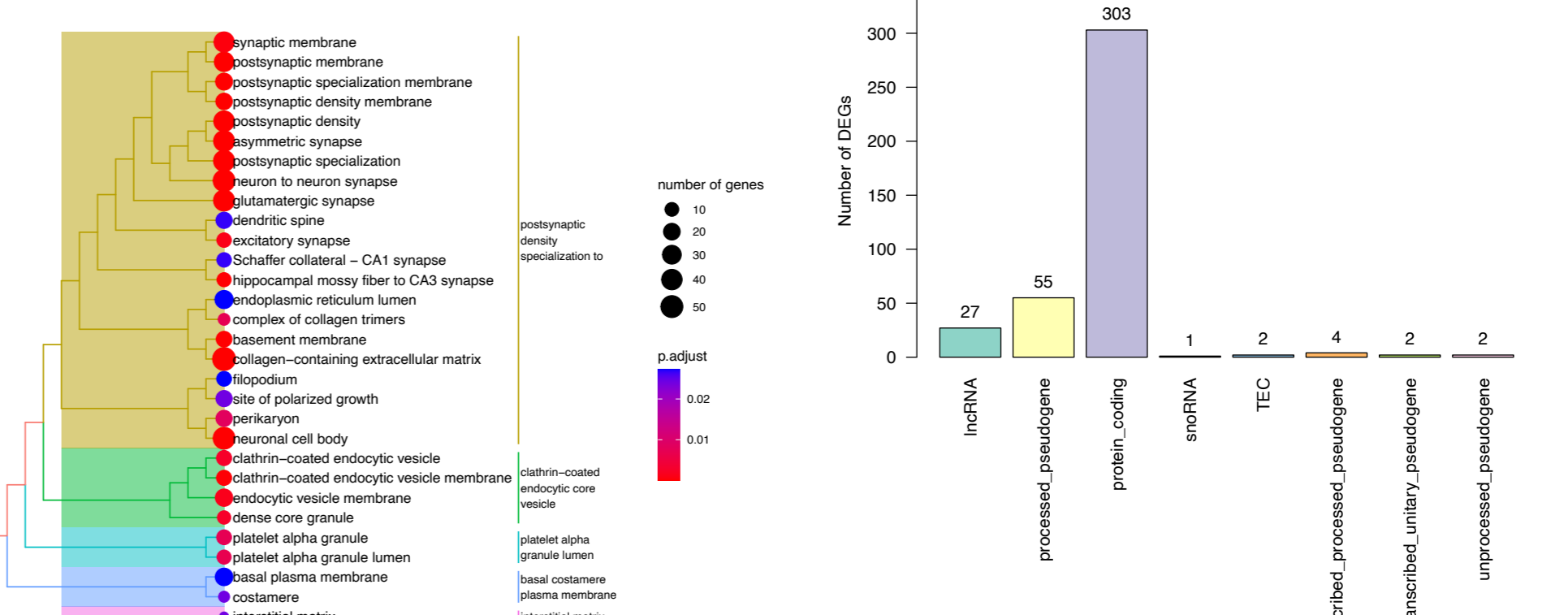


Figure 10. Number of DEGs that emerged after RNA-seq, divided for biotype and FC entity.

Figure 11. Biological Processes Gene Ontology for DEGs

Figure 12. DEGs Gene Biotype.

Conclusions

Preliminary data emphasize a mutation-specific impairment in patients' specific primary fibroblasts, used as pre-clinical experimental model of the disease.

